Effect of laser parameters and compression ratio on particulate emissions from a laser ignited hydrogen engine

Article *in* International Journal of Hydrogen Energy · April 2017

DOI: 10.1016/j.ijhydene.2017.03.074

CITATIONS
13

READS
222

3 authors:

Avinash Kumar Agarwal
Indian Institute of Technology Kanpur
582 PUBLICATIONS **23,244** CITATIONS

SEE PROFILE

Akhilendra Pratap Singh
Indian Institute of Technology Kanpur
102 PUBLICATIONS **3,619** CITATIONS

SEE PROFILE

Anuj Pal
Michigan State University
28 PUBLICATIONS **386** CITATIONS

SEE PROFILE

INTERNATIONAL JOURNAL OF HYDROGEN ENERGY XXX (2017) 1–14

Available online at www.sciencedirect.com

ScienceDirect

journal homepage: www.elsevier.com/locate/he

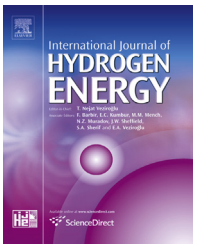

Effect of laser parameters and compression ratio on particulate emissions from a laser ignited hydrogen engine

Avinash Kumar Agarwal[*], *Akhilendra Pratap Singh*, *Anuj Pal*

Engine Research Laboratory, Department of Mechanical Engineering, Indian Institute of Technology Kanpur, Kanpur-208016, India

ARTICLE INFO

Article history:
Received 23 September 2016
Received in revised form
9 March 2017
Accepted 12 March 2017
Available online xxx

Keywords:
Hydrogen
Laser ignition
Particulate number-size distribution
Laser pulse energy
Spark timing
Compression ratio

ABSTRACT

Due to stricter emission legislations and rapid depletion of petroleum resources, research efforts are being made to explore advanced combustion concepts as well as alternative fuels for IC engines, in order to sustain transport sector. Amongst numerous potential options, hydrogen has been identified as one of the most promising alternative fuel candidate. Utilization of hydrogen in IC engines is challenging but it can be successfully achieved by applying laser ignition (LI), which is a novel ignition concept. Researchers have proved that LI parameters significantly affect combustion, performance and emissions characteristics of hydrogen fueled engines; however information about its effect on particulate characteristics is not available in open literature. In this experimental study, particulate emissions from a hydrogen fueled engine using different LI parameters namely laser pulse energy (E) and spark timing (ST), and different compression ratios (CR) have been analyzed. Experiments were carried out in a suitably modified single cylinder prototype engine, which is capable of operating on gaseous fuels and has a LI system. Results showed that increasing engine load resulted in higher particulate number concentration. Increasing E led to formation of higher number of nucleation mode particles (NMP) and accumulation mode particles (AMP). Advancing ST led to higher particulate number concentration, which dominated in the NMP regime therefore the count mean diameter (CMD) of particulate remained relatively smaller. At higher CR, slightly higher particulate concentration was another important observation. Particulate number-size distribution showed greater dominance of CR in AMP regime, compared to NMP regime. This study demonstrated that particulate emissions from laser ignited, hydrogen fueled engines can be controlled by selection of optimum laser parameters and CR of the test engine.

Introduction

Majority of energy consumed in transport sector is of fossil origin, which has led to rapid depletion of non-renewable petroleum resources and increased greenhouse gas (GHG) emissions into the environment. These issues have motivated researchers to explore and develop new and advanced combustion concepts and alternative energy resources for IC engines, which are more efficient and environment friendly. Advanced engine technologies such as common rail direct

* *Corresponding author.*
E-mail address: akag@iitk.ac.in (A.K. Agarwal).

http://dx.doi.org/10.1016/j.ijhydene.2017.03.074
0360-3199/

injection (CRDI) and gasoline direct injection (GDI) have resulted in significantly lower exhaust emissions from modern diesel and gasoline engines respectively. However emissions of different pollutant gases such as oxides of nitrogen (NO_x), and carbon monoxide (CO) as well as particulate matter (PM) are the flip side of their applications in urban areas [1]. Use of after-treatment devices is a seemingly potential solution for emission reduction however it increases complexity and the cost of the vehicles. Hence researchers have explored cleaner alternative fuels such as biofuels, gaseous fuels and synthetic fuels in order to retard the rate of depletion of conventional fossil fuels and improve the ambient air quality. Amongst these alternative fuel candidates, gaseous fuels such as compressed natural gas (CNG), liquefied petroleum gas (LPG), dimethyl ether (DME), etc., are potential alternatives to mineral diesel and gasoline. However presence of carbon atoms in their molecular structure leads to formation of particulate. These particulate consist of an elemental carbon core with several organic compounds, trace metals, polycyclic aromatic hydrocarbons (PAHs) and irritants (such as acrolein, ammonia, acids, fuel vapors, unburnt lubricating oils, etc.) adsorbed onto the surface [2]. Previous studies on engine particulate have shown their harmful health effects [3,4]. Some of the PAHs adsorbed onto particulate surfaces have been proven to be mutagenic and carcinogenic [4].

In such a scenario, a renewable fuel such as hydrogen is an excellent measure for emission compliance requirement of engines used in transport sector. Hydrogen is an odorless, colourless, non-toxic and renewable alternative fuel, which can be produced from water (through electrolysis), from coal and biomass (through gasification) and from natural gas (using steam reforming and other ways) [5]. Researchers have also suggested that the main advantage of hydrogen is that it is a carbon-zero fuel [6]. Hydrogen combustion produces only water vapors as combustion product therefore it can be a potentially promising fuel candidate for next generation sustainable engines. However presence of nitrogen in the air during combustion results in NO_x formation and emissions from a hydrogen fueled engine, which can be reduced largely by exhaust gas recirculation (EGR) [7,8]. Government policies promote research and development of technologies for production, storage and utilization of hydrogen as transport fuel. Several researchers used hydrogen in IC engines and reported significantly improved combustion, performance and emission characteristics. Other researchers explored feasibility of hydrogen in IC engines by using different fuel induction methodologies [9–11]. Gatts et al. [9] reported that addition of hydrogen in conventional fuels led to improved brake thermal efficiency (BTE) and ultra-low emissions at high engine loads. Zhou et al. [10] also suggested that hydrogen improved the engine performance from medium to high engine loads. Singh et al. [12] compared particulate emission characteristics of mineral diesel, gasoline, CNG, HCNG and hydrogen fueled engines and reported that hydrogen fueled engine emitted the lowest particulate numbers as well as particulate mass compared to other test fuels.

Pal et al. [13], Dharamshi et al. [14], and Das [15] reported that pre-ignition and backfire are the main undesirable combustion features of hydrogen, which lead to excessive noise at higher engine loads. This was mainly caused by relatively higher flame speed (2.5–3.25 m/s), wider flammability range (4–75% v/v), lower ignition energy (0.02 mJ) and higher diffusivity of hydrogen compared to other conventional fuels [16]. These issues can be resolved by using an electrode-less ignition system for igniting the fuel-air mixtures in the combustion chamber. Laser ignition (LI) is an electrode-less ignition system, which has great potential in hydrogen engine combustion. In LI, high intensity plasma is created by a short pulsating laser beam, which is focused at the focal point using a converging lens. Plasma generation takes place, when the energy density at the focal point reaches the threshold. Many researchers applied this novel technique to engines and reported its advantages namely lower NO_x emissions, higher BTE and capability to ignite ultra-lean fuel-air mixtures, which could not be ignited by the conventional spark plug [17,18].

In LI system, minimum E, ST, laser beam quality, minimum beam waist size, focal length of the converging lens, and plasma position are important parameters, which affect the ignition characteristics [19]. It has been observed that E required to initiate combustion inside the combustion chamber depends on the in-cylinder pressure and fuel-air ratio [13]. It was also shown that E was directly related to ST because advancing ST resulted in lower in-cylinder pressure [13]. Subramanian et al. [20] carried out engine experiment using hydrogen and investigated the effect of ST on combustion characteristics. They reported that ST affected combustion and NO emissions significantly. In another study carried out by Pal and Agarwal [21], E directly correlated with the engine CR and higher CR resulted in higher in-cylinder pressure, leading to adequacy of lower E [21]. At higher engine loads, richer fuel-air mixtures also required lower E due to faster fuel-air chemical kinetics [13]. DeBoer and Hulet [22] performed experiments in a hydrogen fueled engine at different CRs (5:1 to 12:1) and reported that knocking tendency increased with increasing CR. Mathur and Khajuria [23] reported higher BTE and NO_x emissions at higher CR and suggested that CR was limited by pre-ignition and knocking, especially at higher engine loads. Killingsworth et al. [24] and Mathur and Das [25] also supported the findings of Mathur and Khajuria [23]. These researchers concluded that engine knocking limits the CR and suggested that varying ST could resolve this issue since ST was not limited by knocking.

These studies focused on combustion, performance and gaseous emissions characteristics only. Very few researchers investigated particulate emissions from hydrogen fueled engines. This was mainly due to prevailing mass based particulate emission standards, which amply demonstrated that hydrogen is a cleaner fuel due to significantly lower particulate mass emissions compared to conventional fossil fuels. However particulate numbers emitted by hydrogen fueled engines can't be neglected. Hydrogen fueled engines emit significantly higher nucleation mode particles (D_p < 50 nm) (NMP), which increase potential risk to human health due to their deeper penetration capability in the human respiratory system. Smaller particles have significantly higher probability to be inhaled and get deposited in the respiratory tract, and in the alveolar region of the human respiratory system via the process of diffusion [26]. Toxicological studies have amply demonstrated that fine particles (D_p < 2.5 μm) have higher toxicity per unit mass compared to coarse particles

Please cite this article in press as: Agarwal AK, et al., Effect of laser parameters and compression ratio on particulate emissions from a laser ignited hydrogen engine, International Journal of Hydrogen Energy (2017), http://dx.doi.org/10.1016/j.ijhydene.2017.03.074

(D_p < 10 μm) [27]. Singh et al. [12] suggested that although hydrogen emitted relatively lower particulate mass compared to gasoline, CNG and mineral diesel however the particulate numbers emitted cannot be neglected. Khalek et al. [28] reported that engines with lower particulate emissions favored re-nucleation of lubrication oil additives in the engine exhaust, leading to possibly higher particulate number emissions. Literature shows that hydrogen fueled engines emitted particulate mainly due to incomplete combustion of lubricating oil. Lubricating oil-based metallic additives undergo volatilization during combustion. These vapors condense during cooling of exhaust gas, resulting in formation of different organic and inorganic compounds in the exhaust [28]. Post combustion, these compounds act as soot precursors and promote particulate formation. In hydrogen fueled engines, particulate formation is significantly affected by engine operating conditions, control parameters and test fuel properties. Variations in these parameters control in-cylinder conditions, which directly affect particulate formation.

Since particulate emission characteristics of laser ignited hydrogen fueled engines have not been thoroughly investigated, it becomes necessary to investigate particulate emission characteristics of the LI engines under varying LI parameters and CR. In this study, effect of LI parameters (E and ST) and engine CR on particulate characteristics has been investigated at different engine loads. The experiments were carried out at two Es (12.1 and 16.6 mJ/pulse), three STs (17, 20 and 23° bTDC) and three CRs (10, 11 and 12). All experiments were performed in a hydrogen fueled constant speed single cylinder engine prototype (1500 rpm) at five different engine loads (5, 10, 15, 20 and 25 Nm).

Experimental setup

In this study, experiments were performed in a constant speed compression ignition engine (Kirloskar; DM10), which was modified and converted into a spark ignition engine prototype, capable of operating with gaseous fuels using a LI system. All experiments were performed at 1500 rpm with engine loads varying from 5 to 25 Nm using a transient DC dynamometer (Dynomerk; DC-35). To investigate the particulate emission characteristics at different CR, three pistons having different CR were machined from the original piston (CR: 17.5) and then used in the test engine (Fig. 1). Schematic of the experimental setup is shown in Fig. 1.

Table 1 showed the important modifications done in the original CI engine during the process of developing hydrogen fueled SI engine prototype and the specifications of the test engine used in this study before and after the hardware modifications.

The engine was modified to operate with LI system, which required several hardware modifications (such as intake manifold design modifications, CR changes, etc.) along with development and installation of electronic circuit to control port fuel injector and ST. To measure the mass flow rate of hydrogen, a Coriolis force based fuel mass flow meter (Emerson; CMF010M) was used, which was capable of

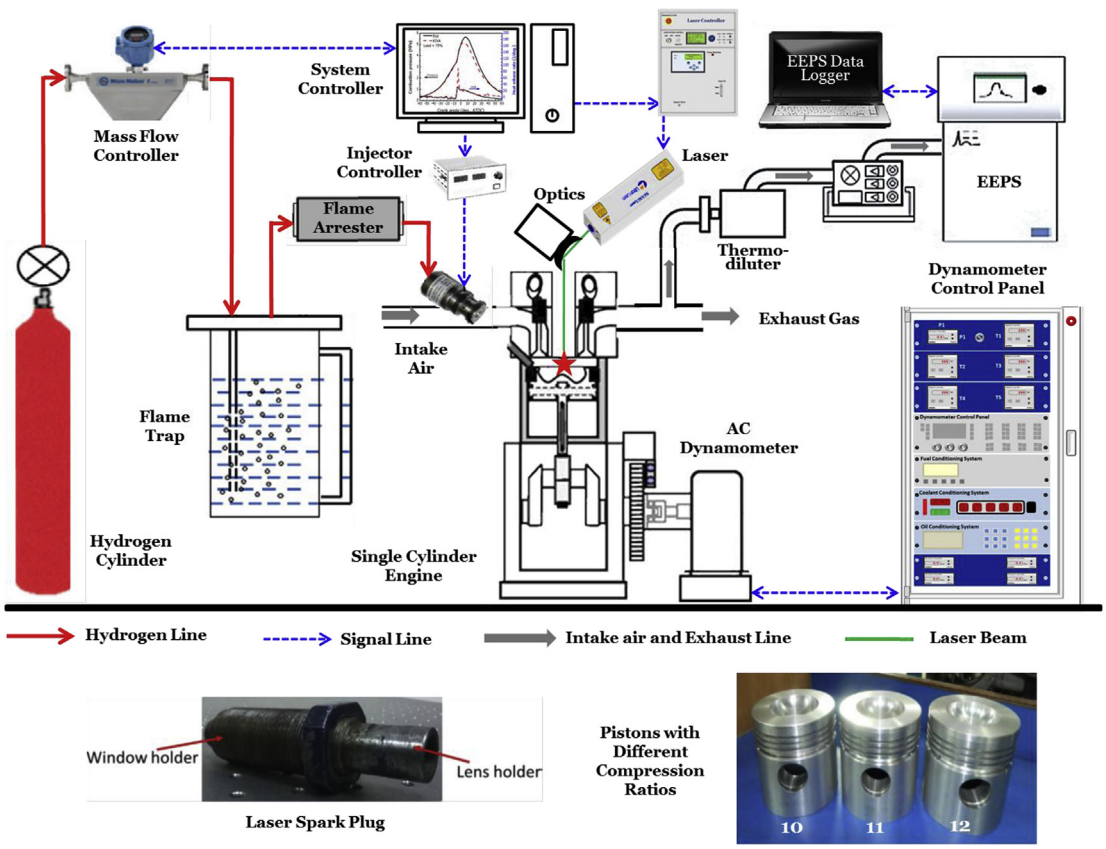

Fig. 1 – Schematic of hydrogen fueled laser ignited single cylinder engine.

Please cite this article in press as: Agarwal AK, et al., Effect of laser parameters and compression ratio on particulate emissions from a laser ignited hydrogen engine, International Journal of Hydrogen Energy (2017), http://dx.doi.org/10.1016/j.ijhydene.2017.03.074

Table 1 – Specifications of the prototype test engine before and after the modifications.

Specifications	Original engine (CI)	Hydrogen fueled laser ignited engine (SI)
Make/model	Kirloskar/DM-10	Kirloskar/ERL-3
Fuel induction type	Direct injection	Port fuel injection
Number of cylinder/s	One	One
Ignition type	Compression ignition	Laser spark ignition
Spark timing (°bTDC)	NA	17, 20 and 23
Bore (mm)/stroke (mm)	102/116	102/116
Displaced volume (cc)	948	948
Compression ratio	17.5	10, 11 and 12
Connecting rod length (mm)	232	232
Intake air	Naturally aspirated	Naturally aspirated
Inlet valve opening time	4.5° BTDC	4.5° BTDC
Inlet valve closing time	35.5° ABDC	35.5° ABDC
Exhaust valve opening time	35.5° BBDC	35.5° BBDC
Exhaust valve closing time	4.5° ATDC	4.5° ATDC
Cooling system	Water cooled	Water cooled

measuring fuel mass flow rates up to 30 kg/h. Development of suitable fuel injection system was the most important task for developing hydrogen fueled engine prototype because hydrogen had very fast flame speed, which resulted in higher probability of backfire in the intake manifold. Hydrogen requires very low ignition energy therefore backfire can potentially occur due to hot spots present in the combustion chamber [29]. This could be avoided by employing suitable fuel injection strategy, which reduces intensity of such hot spots in the combustion chamber. In order to avoid this unwanted phenomenon, several safety measures were taken in the experiment such as design and fabrication of two safety devices namely (i) flame arrestor, and (ii) flame trap. Flame trap was used for water quenching of flames traveling in backward direction, while flame arrester was used to diminish flame propagation by quenching. Downstream of these safety devices, a high volume flow rate solenoid injector (Alternative Fuel Systems; Gs-60-05-5 H) was used to inject hydrogen into the intake manifold of the engine. This fuel injector was controlled by a dedicated electronic circuit, which was capable of controlling all injection parameters such as start of injection timing, injection duration (fuel injection quantity) and injection lag. LI system being the most important part of this experimental setup, consisted of a Q-switched Nd:YAG laser (Litron; Nano L-200-30), a collimating unit (a combination of diverging and collimating lenses), a beam reflector and a laser spark plug. This laser was capable of delivering up to 200 mJ/pulse energy at fundamental wavelength (1064 nm). To control E, an external optical attenuator was installed in front of the laser head. All parameters of the laser such as E and laser frequency were controlled by the laser controller. This laser controller was a separate unit, which also supplied cooling water to the laser in order to avoid excessive heating of the laser crystals. For performing experiments, E was varied, while maintaining the flash lamp voltage constant. The collimating unit was used to increase the diameter of the laser beam, which was generated from the laser head. The laser beam was then directed towards the laser spark plug using a beam reflector (mirror). The laser spark plug was installed in the cylinder head (Fig. 1) in place of fuel injector of the unmodified engine. To align the laser beam and make it follow the axis of laser spark plug, beam reflector angle was suitably adjusted. To avoid gas leakage from the combustion chamber, a sapphire window (5 mm thick) was installed at the bottom of the laser spark plug, which acted as an interface between the burning gases of the combustion chamber and the lens. To control ST of the laser plasma, a separate laser triggering circuit was designed, which takes input from the top dead center (TDC) sensor fitted on the engine camshaft.

For measurement of particle number-size distribution, an engine exhaust particle sizer (EEPS) spectrometer (TSI; 3090) was used. This instrument provides high temporal resolution as well as reasonable size resolution using multiple detectors, which work in parallel. EEPS can measure particles in sizes ranging from 5.6 to 560 nm with a maximum concentration of 10^8 particles/cm^3 in the engine exhaust. Sometimes when the concentration of particles emitted by the engine exceeds this limit, then a rotating disk thermo-diluter (Matter Engineering; MD19-2E) was used to dilute the exhaust gas prior to entry into the EEPS. To remove large size particles ($D_p > 1$ μm), particulate enter the EEPS through a cyclone [30].

Results and discussion

This study compares the particulate characteristics of laser ignited hydrogen fueled engine using different LI parameters (E and ST) and different CR. Experiment were performed at two different Es (12.1 and 16.6 mJ/pulse), three STs (17, 20 and 23° bTDC) and three CRs (10, 11 and 12). 16.6 mJ/pulse was the maximum E that could be generated by the laser using a 2.5 mm diameter aperture and 12.1 mJ/pulse was the minimum E, which was capable of generating laser plasma with 100% probability. Further reduction in E reduced plasma formation probability, resulting in engine misfire as well as rough engine operation. All experiment were carried out at constant engine speed (1500 rpm) at five different engine loads/torques (5, 10, 15, 20, and 25 Nm). Exhaust gas sampling was done using EEPS, only after thermal stabilization of the engine. To avoid measurement errors, distributions of particulate samples were recorded for one minute (at a frequency 1 Hz) and the average data set of these 60 measured data sets was used for comparing the particulate characteristics. For detailed analysis of particulate characteristics, results were analyzed for number-size, surface area-size and mass-size distributions of particulate.

Particulate number-size distribution

Fig. 2 shows the number-size distribution of particulate emitted by LI hydrogen fueled engine at different Es, STs and CRs.

Please cite this article in press as: Agarwal AK, et al., Effect of laser parameters and compression ratio on particulate emissions from a laser ignited hydrogen engine, International Journal of Hydrogen Energy (2017), http://dx.doi.org/10.1016/j.ijhydene.2017.03.074

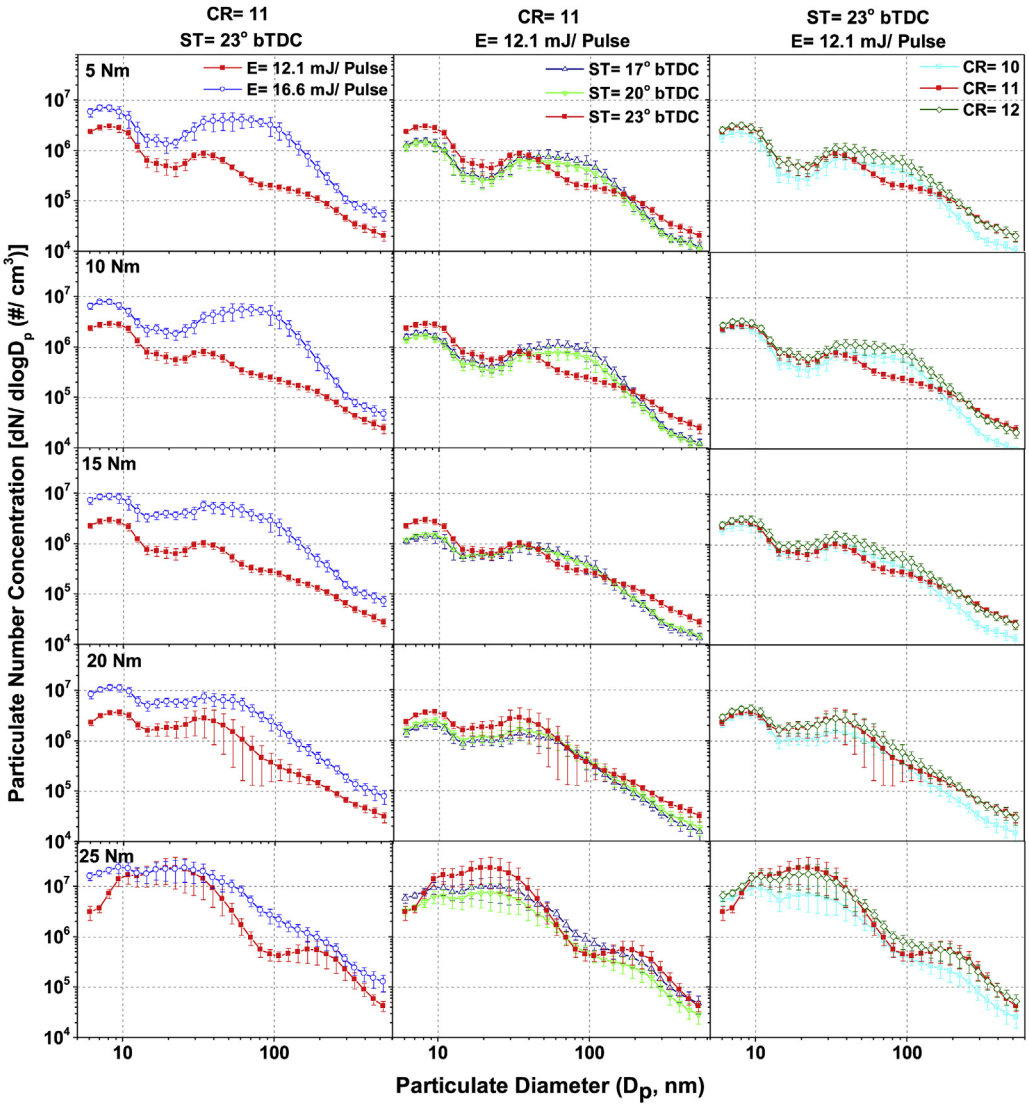

Fig. 2 – Number-size distributions of particulate emitted by LI hydrogen fueled engine at different engine loads, Es, STs and engine CRs.

First set of experiments were performed at different Es (12.1 and 16.6 mJ/pulse) (Column 1 of Fig. 2). During these experiment, ST and CR were maintained constant at 23° bTDC and 11 respectively. Results showed that particulate number-size distributions of the laser ignited hydrogen fueled engine had two peaks corresponding to NMP and accumulation mode particles (AMP). Singh et al. [12] also presented similar results for hydrogen fueled SI engine however particulate number concentration was slightly lower compared to LI system. At both Es, particulate number concentrations increased with increasing engine load. Particulate characteristics at different Es clearly indicated that increasing E resulted in significantly higher particulate number concentrations. Particulate number-size distributions showed that the concentrations of both NMP and AMP were higher at higher E. In presence of higher E, ignition quality improved, which resulted in superior combustion. This led to higher in-cylinder temperature, which enhanced the pyrolysis of lubricating oil present on the engine liner surfaces. Variations in particulate number-size distributions at different Es showed slightly different pattern at higher engine loads. With increasing engine load, maximum concentration of AMP at higher E (16.6 mJ/pulse) shifted downwards and maximum concentration of NMP shifted upwards. However at lower E (12.2 mJ/pulse), maximum concentration of AMP increased slightly but maximum concentration of NMP remained almost constant (except at 25 Nm). This shows the effect of E and engine load on particulate formation. At lower E, increasing engine load led to higher in-cylinder temperatures, which resulted in slightly higher NMP number concentration. At higher E, particulate formation due to increasing engine load became less dominant compared to higher number of nuclei formation because of superior combustion. This resulted in higher number of NMP formation. Also, at higher E, significantly faster combustion of hydrogen (highly diffusive) led to relatively shorter combustion duration. Furthermore, at higher E,

Please cite this article in press as: Agarwal AK, et al., Effect of laser parameters and compression ratio on particulate emissions from a laser ignited hydrogen engine, International Journal of Hydrogen Energy (2017), http://dx.doi.org/10.1016/j.ijhydene.2017.03.074

energy density of plasma increased leading to relatively higher heat release rate (HRR). This was the main reason for significantly higher NMP at higher E. Lower combustion duration also inhibited coagulation of NMP, which resulted in relatively lower AMP number concentration. At 25 Nm, difference between particulate number-size distributions of both Es decreased. This was mainly due to significantly higher HRR because of presence of higher hydrogen quantity in the combustion chamber, which was more effective than the combustion improvement due to higher E. At higher engine loads, uncertainty in particulate number concentration emitted at lower E was slightly higher compared to lower engine loads. This was mainly due to dominating effect of engine load and E. In case of lower E, effect of engine load was dominant, which led to knocking and resulted in greater uncertainty in particulate number concentration.

Second set of experiment were performed at different STs (17, 20 and 23° bTDC) (Column 2 of Fig. 2). During these experiment, CR and E were maintained constant at 11 and 12.1 mJ/pulse respectively. Results showed that particulate number concentrations increased with increasing engine load and were slightly higher in case of advanced ST. Advancing ST resulted in higher HRR, leading to higher in-cylinder temperatures. This enhanced the pyrolysis of lubricating oil, resulting in higher number concentration of particulate. Relatively lower combustion duration at advanced STs was another important reason for higher particulate number concentrations. With advancing ST, NMP number concentration increased and AMP number concentration decreased slightly. This was due to superior combustion at advanced STs, which led to higher HRR and shorter combustion duration. Lack of time available for coagulation of NMP resulted in lower AMP number concentration. Difference in AMP number concentration decreased with increasing engine load. Compared to advanced ST (23° bTDC), retarded STs (17 and 20° bTDC) showed relatively higher AMP number concentration. This indicated greater coagulation tendency of particulate at retarded STs. For all STs, increasing engine load resulted in higher AMP number concentration. In addition, position of peak AMP number concentration shifted towards smaller size. This showed greater possibility of NMP formation at higher engine loads. Similar to previous observations, 25 Nm load resulted in significantly higher particulate number concentration, in which NMPs dominated over AMPs.

Third set of experiment were performed at different CRs (10, 11 and 12) (Column 3 of Fig. 2). During these experiment, ST and E were maintained constant at 23° bTDC and 12.1 mJ/pulse respectively. This set of experiment also showed similar observations as that of increasing engine load, resulting in higher particulate number concentrations. Comparison of particulate number-size distributions at different CRs showed that increasing CR led to slightly higher particulate number concentrations, especially in the AMP regime. NMP distributions increased slightly with increasing CR however differences between peaks corresponding to NMP number concentrations were almost negligible. Increasing CR resulted in higher in-cylinder pressure, which enhanced incomplete combustion of lubricating oil. This led to higher number concentrations of both NMPs as well as AMPs. Effect of engine load on particulate characteristics was slightly lower at lower CRs. This was mainly due to lower in-cylinder temperatures at relatively lower CR. This can be clearly seen at higher engine loads, where particulate concentration corresponding to CR = 10 was significantly lower compared to CR = 11 and 12. At lower engine loads, CR = 10 resulted in slightly higher AMP number concentration compared to CR = 11. This was attributed to relatively longer combustion duration, which provided sufficient time for coagulation of NMPs, leading to higher AMP number concentration.

Nucleation and accumulation mode particulate number

Fig. 3 shows the variation of NMP and AMP number concentrations w.r.t. engine loads at different Es, STs and CRs. Relative concentrations of NMPs and AMPs are important because size of particulate directly affect their toxic potential as well as their health risk potential [26,27].

Fig. 3 showed that increasing engine load resulted in higher NMP and AMP number concentrations. At higher E, variations in AMP showed slightly irregular pattern with AMP concentrations varying from ~2×10^7 to 3×10^7 particles/cm^3. Singh et al. [12] also reported similar results for SI hydrogen fueled engine. At all engine loads, NMP number concentrations were significantly higher compared to AMP number concentrations. These observations validated the findings of particulate number-size distributions (Fig. 2). Results showed that increasing E resulted in significantly higher NMP and AMP number concentrations. Differences between number concentrations at different Es decreased slightly at the highest engine load. This was mainly due to dominance of higher fuel quantity compared to higher E, which led to significantly higher in-cylinder temperatures and promoted particulate formation. At lower E, NMP number concentration varied from ~2×10^7 to 2×10^8 particles/cm^3, however at higher E, NMP number concentration reached up to ~3×10^8 particles/cm^3 of the exhaust gas.

Fig. 3 also showed that advancing ST resulted in slightly higher NMP number concentration however at maximum engine load, 20° bTDC ST showed lowest NMP number concentration. This observation revealed importance of optimum ST for hydrogen fueled engine, which changed with the engine load. Contrary to variations in NMP, advanced ST resulted in slightly lower AMP number concentration. This was primarily due to faster combustion, which resulted in lower coagulation of NMP and led to lower AMP number concentration. Amongst all three STs, 20° bTDC ST showed the best particulate characteristics. Furthermore, Fig. 3 showed that increasing CR resulted in higher NMP and AMP number concentrations. At higher CR, minimum E reduced slightly due to relatively higher in-cylinder pressure. Therefore E = 12.1 mJ/pulse led to intense ignition inside the combustion chamber, resulting in superior combustion, which promoted incomplete combustion of lubricating oil at the highest engine load (25 Nm). These findings showed that increasing CR improved combustion, performance and emissions characteristics [21] however it also led to higher particulate emissions. Therefore, optimum CR should be selected keeping in mind the trade-off between engine performance and emissions characteristics of hydrogen fueled engine.

Please cite this article in press as: Agarwal AK, et al., Effect of laser parameters and compression ratio on particulate emissions from a laser ignited hydrogen engine, International Journal of Hydrogen Energy (2017), http://dx.doi.org/10.1016/j.ijhydene.2017.03.074

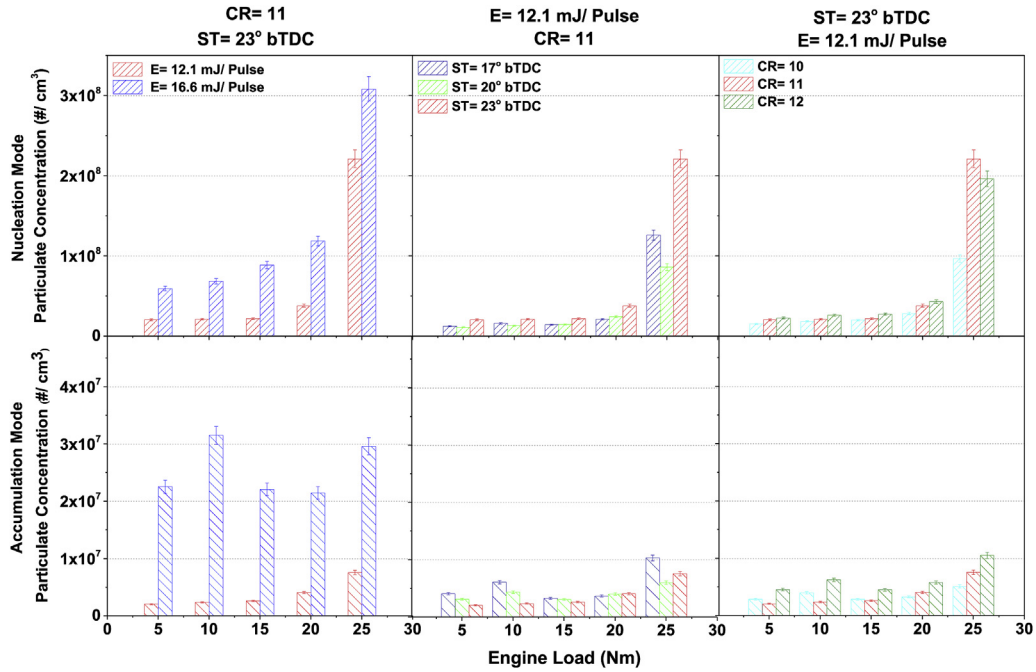

Fig. 3 – Number concentration of nucleation and accumulation mode particulate emitted by LI hydrogen fueled engine at different engine loads, Es, STs and engine CRs.

Total particulate number and count mean diameter

Fig. 4 shows the variations in total particulate number (TPN) concentration and count mean diameter (CMD) of particulate emitted by LI hydrogen fueled engine. Increasing engine load resulted in higher TPN concentration. This trend was observed for all engine operating conditions. Similar trends were also reported by Singh et al. [12]. Results showed that increasing E resulted in significantly higher TPN concentration. This was mainly due to more intense plasma ignition,

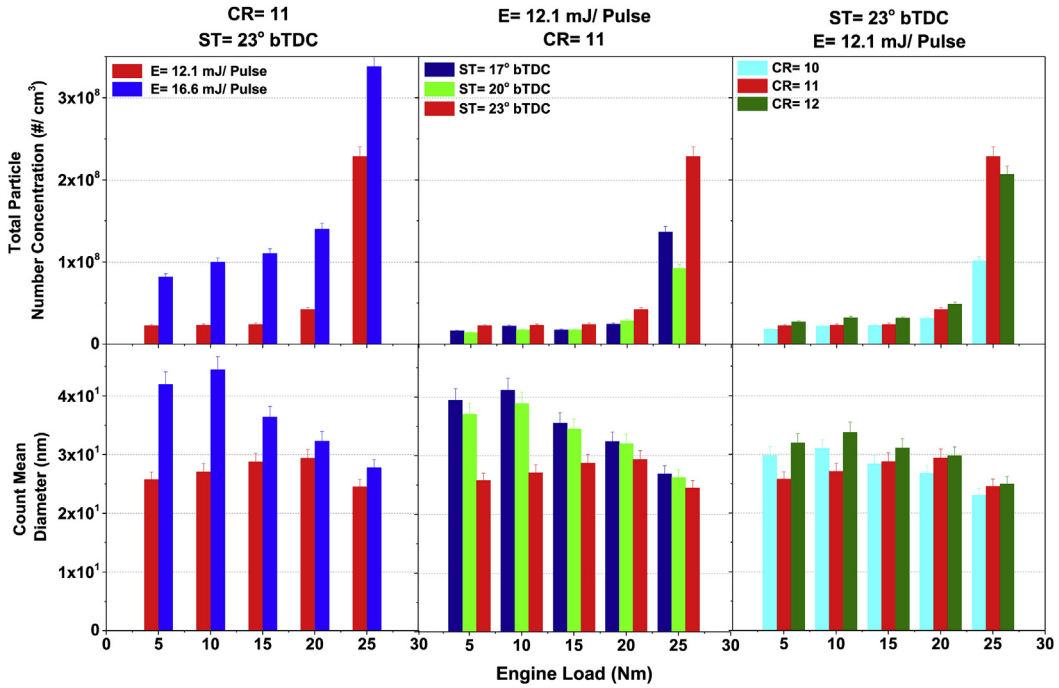

Fig. 4 – TPN and CMD of particulate emitted by LI hydrogen fueled engine at different engine loads, Es, STs and engine CRs.

Please cite this article in press as: Agarwal AK, et al., Effect of laser parameters and compression ratio on particulate emissions from a laser ignited hydrogen engine, International Journal of Hydrogen Energy (2017), http://dx.doi.org/10.1016/j.ijhydene.2017.03.074

resulting in superior combustion. At higher E, laser beam penetrated relatively deeper into the plasma compared to lower E, leading to superior ignition and combustion, which enhanced lubricating oil pyrolysis. At lower E, TPN concentration varied from ~3 × 10^8 to 2.5 × 10^8 particles/cm^3 of the exhaust gas. Singh et al. [12] reported slightly lower TPN from SI hydrogen fueled engine. Advanced ST resulted in slightly higher TPN concentration however at the highest engine load, 20° bTDC ST showed lowest TPN concentration. This was mainly due to two counter effects. At advanced ST (23° bTDC), higher HRR resulted in higher TPN, whereas at retarded ST (17° bTDC), longer combustion duration promoted re-nucleation of lubrication oil additive based particulate in the exhaust, leading to higher TPN concentration [28]. Increasing CR also resulted in higher TPN concentration. At lower loads, effect of CR was less dominant however at higher engine loads, increasing CR led to significantly higher TPN concentration. At maximum engine load (25 Nm), slightly lower TPN concentration at CR = 12 was an important observation. This was mainly due to reduction in NMP number concentration.

Fig. 4 shows the variations of CMD at different Es, STs and CRs. CMD was calculated from the particulate number-size distribution using the following equation:

$$CMD = \frac{n_1 d_1 + n_2 d_2 + n_3 d_3 + \cdots + n_n d_n}{n_1 + n_2 + n_3 + \cdots + n_n}$$

Here n_i is the particulate number concentration corresponding to diameter D_i.

CMD represents the average size of particulate emitted by the engine. Higher CMD showed dominance of larger particles in particulate number-size distribution and lower CMD indicated dominance of relatively smaller particles. Previous studies related to health effects of particulate indicated that smaller particles are relatively more harmful to the human health compared to larger particles. Therefore engines emitting particulate of smaller CMD are potentially more hazardous to the human health.

Results obtained show that increasing engine load leads to slightly higher CMD of the particulate, however at higher engine loads, CMD reduced due to dominance of NMP compared to AMP. Increasing E resulted in slightly higher CMD of particulate, mainly due to higher AMP number concentration because of coagulation of NMP. At higher E, effect of engine load dominated at relatively lower engine load (~15 Nm), whereas at lower E, dominance was observed at ~20 Nm. This indicated that variation in NMP was more dominant at higher E. CMD varied from ~20 to 40 nm for different engine loads in LI hydrogen fueled engine, which was lower than mineral diesel and gasoline fueled engines [12]. Advancing ST resulted in lower CMD of particulate. At advanced STs, higher HRR and lower combustion durations reduced coagulation of particulate, leading to significantly higher NMPs. Increasing CR showed an interesting trend of variations in CMD of particulate. At lower engine loads (up to 10 Nm), CR = 11 resulted in the lowest CMD of particulate, whereas at higher engine load, CR = 12 showed the highest CMD of particulate. This was mainly due to two factors. At lower engine loads, increasing CR from 10 to 11 resulted in higher NMP number concentration however at CR = 12, coagulation of NMP enhanced due to relatively longer combustion duration. At higher engine loads, higher NMP number concentration resulted in significantly lower CMD of particulate. Amongst all three CRs, CR = 10 yielded lowest CMD at higher engine loads. This was mainly due to significantly lower TPN compared to CR = 11 and 12.

Particulate surface area-size distribution

Particulate toxicity is significantly affected by the particulate surface area. Particulate surface provides site for adsorption of volatile hydrocarbon species and PAHs, which are responsible for the toxic character of particulate. These particulate enter into the human body through the respiratory system, leading to different life threatening diseases. Particulate surface area-size distribution is calculated from the particulate number-size distribution, and all particles are assumed to be spherical [30]. The following equation is used for calculation of particulate surface area:

$$dS = dN \cdot (D_p)^2$$

Here dS is the surface area of particles of size range having mean diameter D_p and dN is the number concentration of particulate with mean diameter Dp.

Fig. 5 showed the surface area-size distributions of particulate emitted by LI hydrogen fueled engine at different engine loads, Es, STs and CRs. In all conditions, particulate surface area distribution increased with increasing engine load. This was mainly due to increased particulate number concentration, mainly in the AMP regime, which contributed significantly to the particulate surface area. Also in all conditions, particulate surface area increased with increasing particulate size. Larger particulate are less harmful to the human health because they get trapped in the upper section of the respiratory system, thereby reducing potential health risks.

Surface area of particulate emitted at higher E (16.6 mJ/pulse) was significantly higher compared to lower E (12.1 mJ/pulse). At lower engine loads, peaks of particulate surface area was in AMP size regime, however at the highest engine load, two peaks in the particulate surface area-size distribution corresponding to NMP and AMP particulate were observed. This showed significant contribution of NMP to particulate surface area, which promoted combination of two harmful effects, namely higher surface area available for adsorption and lower particulate size that increases their capacity to penetrate deeper into the respiratory system. Particulate surface area-size distributions at different STs showed that advanced ST resulted in higher surface area distribution in the NMP size regime, whereas particulate surface area-size distribution were higher in AMP size regime for retarded ST. With increasing engine load, peak of particulate surface area corresponding to AMPs shifted towards NMPs. This tendency was more dominant at advanced ST compared to retarded ST. This was mainly due to significant increase in NMP number concentration at higher engine loads. With increasing CR, particulate surface area-size distribution was mainly affected in the AMP size regime. In NMP size regime, particulate surface area-size distributions remained almost constant at different CRs. At CR = 11, particulate surface area-size distribution was the lowest in the AMP size regime, which increased with increasing engine load. At higher engine loads, particulate

Please cite this article in press as: Agarwal AK, et al., Effect of laser parameters and compression ratio on particulate emissions from a laser ignited hydrogen engine, International Journal of Hydrogen Energy (2017), http://dx.doi.org/10.1016/j.ijhydene.2017.03.074

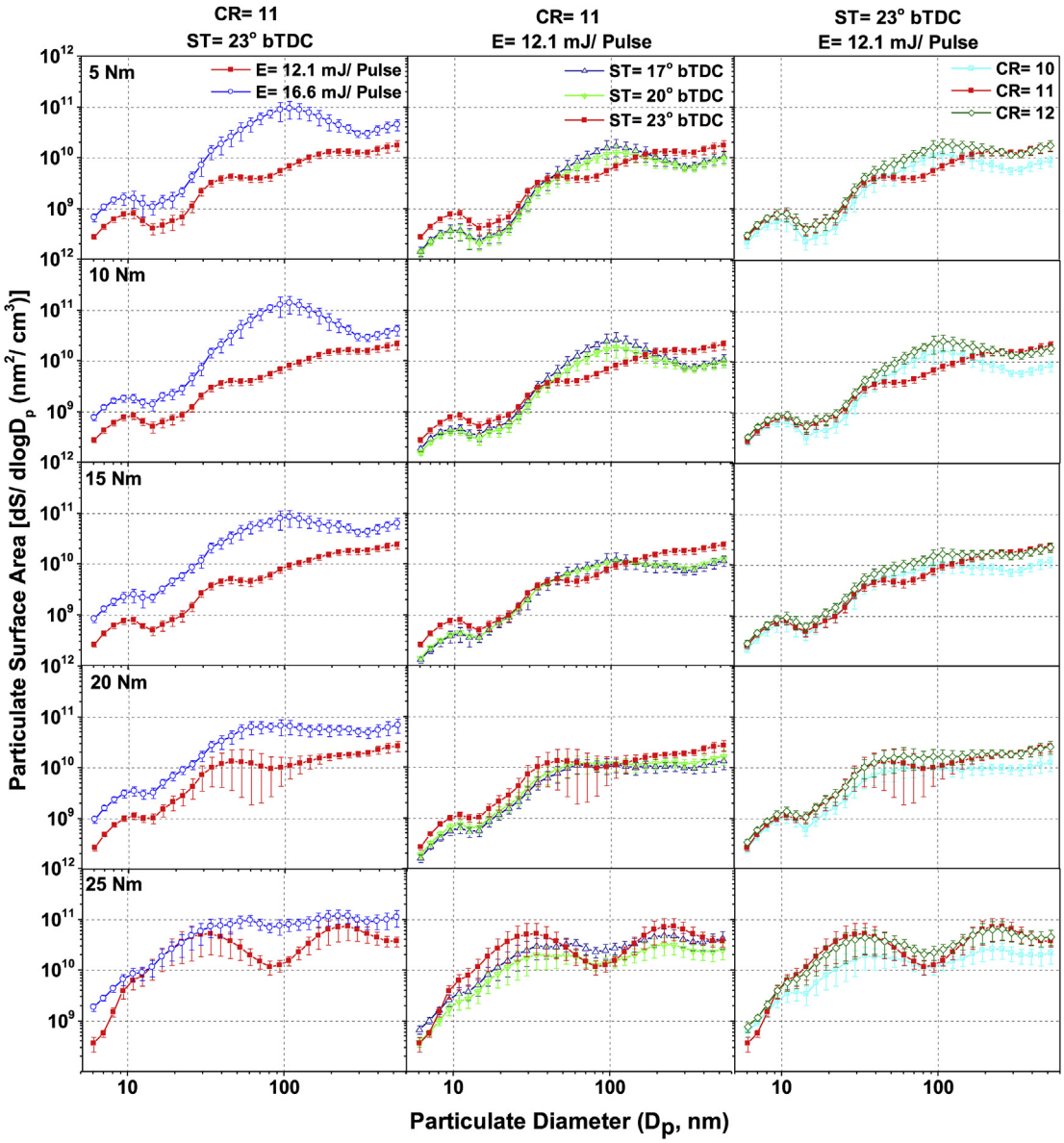

Fig. 5 – Surface area-size distribution of particulate emitted by LI hydrogen fueled engine at different engine loads, Es, STs and engine CRs.

surface area-size distribution increased with increasing CR in both NMP as well as AMP regimes. Overall, particulate surface area-size distributions at different LI parameters and CR showed that selection of suitable combination of these parameters can effectively control particulate surface area and reduce their toxic potential.

Particulate mass-size distribution

Particulate mass is an important measure, which affects the human health risk potential and environmental impact. Lighter particles are more harmful than heavier particles due to their longer retention time in the atmosphere. Researchers have proved that heavier particles have higher settling velocity, which reduces the possibility of them being absorbed into the respiratory system during breathing. Particulate volume was calculated from the number-size distribution of particulate, assuming them to be spherical [30,31]. For calculating particulate mass from the particulate volume, a constant density of particulate (1 g/cm^3) was assumed and used in the calculations by various researchers [30–33]. Fig. 6 shows the particulate mass-size distributions of particulate emitted by the laser ignited hydrogen fueled engine at different engine loads, Es, STs and CRs.

From this figure, it could be observed that particulate mass-size distribution increased with increasing engine load. This increment was more in AMP size regime, whereas particulate mass-size distribution in the NMP size regime remained almost constant. Contrary to number-size and surface area-size distributions of particulate at different engine loads, particulate mass corresponding to AMPs was always higher compared to NMPs. This is the main reason why particulate characteristics of hydrogen fueled engines have

Please cite this article in press as: Agarwal AK, et al., Effect of laser parameters and compression ratio on particulate emissions from a laser ignited hydrogen engine, International Journal of Hydrogen Energy (2017), http://dx.doi.org/10.1016/j.ijhydene.2017.03.074

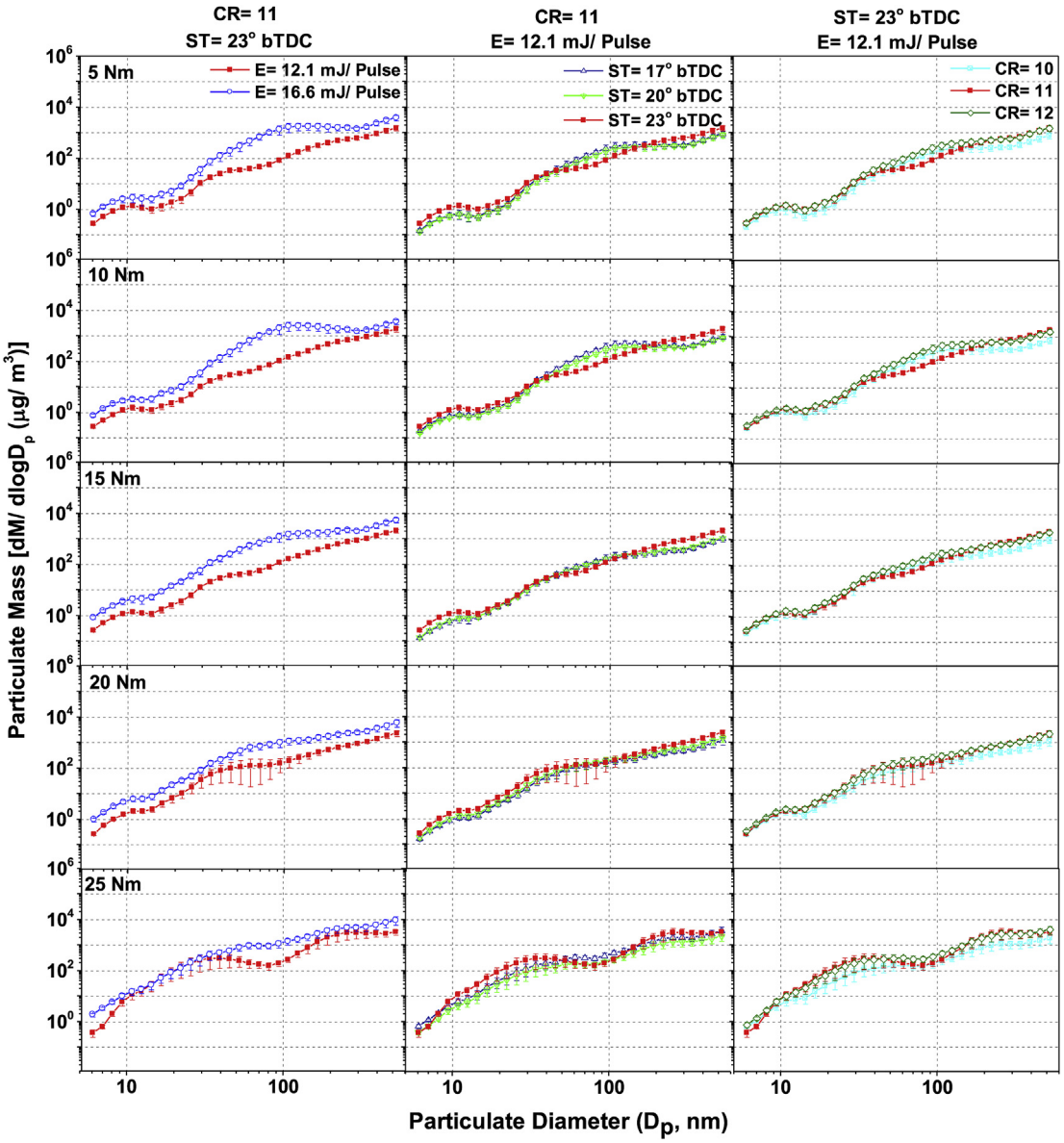

Fig. 6 – Mass-size distribution of particulate emitted by LI hydrogen fueled engine at different engine loads, Es, STs and engine CRs.

not been studied thoroughly. At the highest engine load (25 Nm), hydrogen combustion resulted in significantly higher particulate mass corresponding to NMP. This was mainly due to presence of greater fuel quantity at higher engine load, which promoted pyrolysis of lubricating oil due to higher in-cylinder temperatures (higher HRR). Results also showed that particulate mass at higher E was significantly higher compared to lower E. This was mainly due to higher HRR, which resulted in enhanced pyrolysis of lubricating oil, leading to higher particulate mass. The difference between particulate mass-size distributions at different Es decreased slightly with increasing engine load. This was attributed to dominance of fuel quantity over superior combustion due to better ignition characteristics. Additionally, Fig. 6 showed that particulate mass slightly increased in both NMP and AMP regimes with advancing ST. This was mainly due to coagulation of smaller particles due to presence of significantly higher number of particulate at advanced STs, which contributed to the particulate mass. Therefore even though NMPs comprised of 60–70% of total particulate emissions, it didn't contribute much to the particulate mass. Fig. 6 also shows that increasing CR resulted in slightly higher particulate mass, however CR = 11 resulted in lower particulate mass corresponding to AMPs. This showed that slightly lower coagulation of smaller particles occurred at CR = 11. This was mainly due to trade-off between reduction in combustion duration and significant increment in NMPs at CR = 11.

Overall, particulate mass-size distributions at different LI parameters and engine operating conditions showed that

Please cite this article in press as: Agarwal AK, et al., Effect of laser parameters and compression ratio on particulate emissions from a laser ignited hydrogen engine, International Journal of Hydrogen Energy (2017), http://dx.doi.org/10.1016/j.ijhydene.2017.03.074

particulate mass was not significantly affected by ST and CR. These parameters affected particulate number concentrations though. However total particulate generated by the pyrolysis of lubricating oil were not significantly affected by these parameters.

Nucleation mode, accumulation mode and total particulate mass

Fig. 7 showed the particulate mass corresponding to NMPs and AMPs. It was calculated by integrating the particulate mass corresponding to these size ranges. Results showed that particulate mass corresponding to both NMPs and AMPs increased with increasing engine load.

Rate of increase in particulate mass was relatively lower for AMPs compared to NMPs. Contrary to NMP and AMP number concentrations, mass distribution showed slightly different trend. It was observed that particulate mass corresponding to AMPs (~10^4 μg/m^3 of exhaust gas) was significantly higher compared to NMPs (~10^3 μg/m^3 of exhaust gas). This was mainly due to higher contribution of larger particles to the particulate mass. NMP and AMP mass were significantly higher at higher E. This indicated that total lubricating oil pyrolysis was prominent at higher E due to superior combustion. Fig. 7 also showed that particulate mass corresponding to NMP and AMP were not significantly affected by variation in ST. At each engine load, advanced ST resulted in almost equal NMP mass, while AMP mass slightly increased due to coagulation of smaller particles. Increasing CR resulted in higher particulate mass corresponding to both NMPs and AMPs. This showed that increasing CR led to pyrolysis of higher quantity of lubricating oil. Amongst the three CRs,

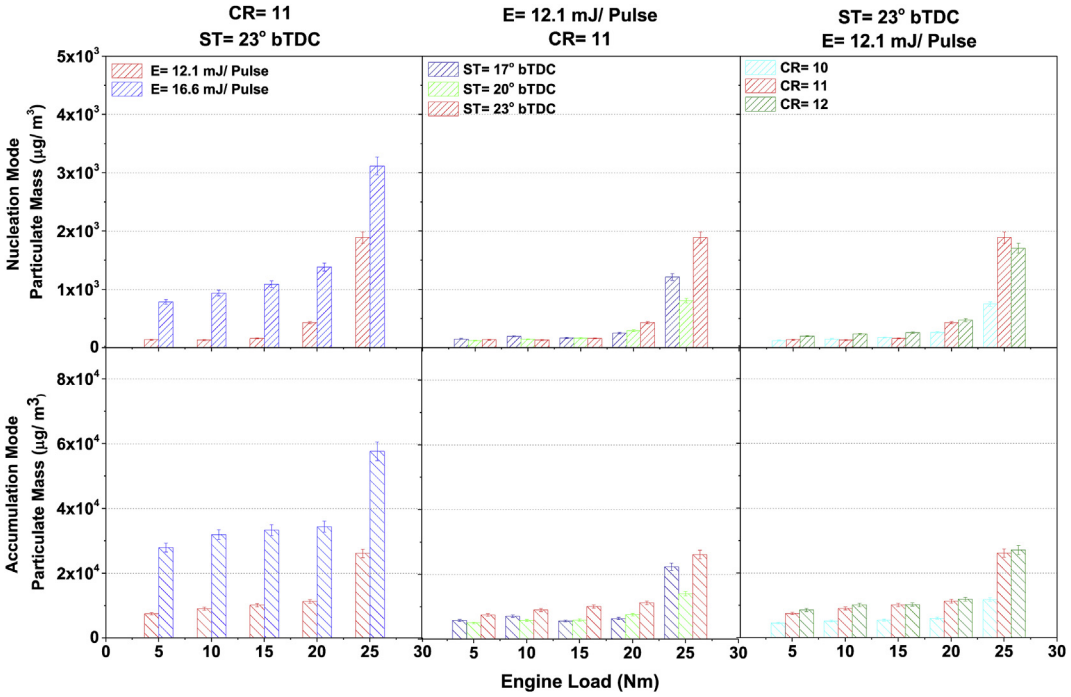

Fig. 7 – Mass of nucleation and accumulation mode particulate emitted by LI hydrogen fueled engine at different engine loads, Es, STs and engine CRs.

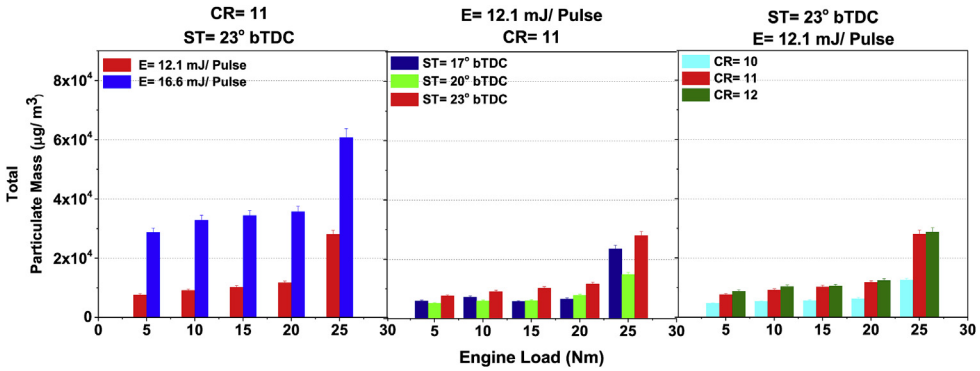

Fig. 8 – Total particulate mass emitted by LI hydrogen fueled engine at different engine loads, Es, STs and engine CRs.

Please cite this article in press as: Agarwal AK, et al., Effect of laser parameters and compression ratio on particulate emissions from a laser ignited hydrogen engine, International Journal of Hydrogen Energy (2017), http://dx.doi.org/10.1016/j.ijhydene.2017.03.074

CR = 10 showed slightly lower particulate mass, whereas particulate mass corresponding to CR = 11 and 12 didn't show any significant difference.

Fig. 8 shows the total particulate mass (TPM) emitted by LI hydrogen fueled engine at different engine loads, Es, STs and CRs. Results showed that TPM increased with increasing engine load. At all conditions, TPM was significantly higher at 25 Nm engine load due to presence of higher fuel quantity, which led to higher HRR and resulted in enhanced pyrolysis of lubricating oil. TPM varied up to ~10^4 μg/m^3 of the exhaust gas, which was significantly lower compared to mineral diesel and gasoline [12].

TPM at E = 16.6 mJ/pulse was significantly higher compared to E = 12.1 mJ/pulse. This observation was in agreement with the findings of particulate mass-size distributions. Advancing ST resulted in slightly higher TPM, though amongst the three ST's, ST = 20° bTDC resulted in relatively lower TPM at highest engine load. Increasing CR resulted in higher TPM, but differences in the TPM at CR = 11 and 12 were very low. Amongst the three CRs, CR = 10 resulted in significantly lower TPM, mainly due to lower in-cylinder temperature, which resulted in lower pyrolysis of the lubricating oil.

Selection of suitable ST and CR

Results of this study clearly indicated that particulate emissions from LI hydrogen fueled engine were significantly affected by LI parameters, namely E and ST. This section relates LI parameters with engine CR so that suitable LI parameters can be obtained for different engines. This analysis has been carried out at constant engine load (15 Nm).

Fig. 9 showed the variation of TPN at different Es and STs. At lower E, TPN was not affected by ST however at higher E, TPN slightly increased with advancing ST. This showed that particulate emissions from LI hydrogen fueled engine can be reduced by retarding ST at higher E. Retarded ST resulted in lower HRR, which in-turn reduced the effect of higher E and led to lower particulate formation.

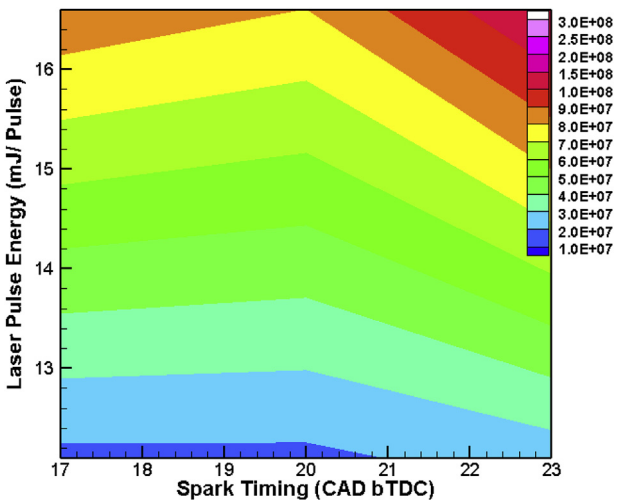

Fig. 9 – Selection of suitable STs and E for lower total particulate numbers emitted by LI hydrogen fueled engine.

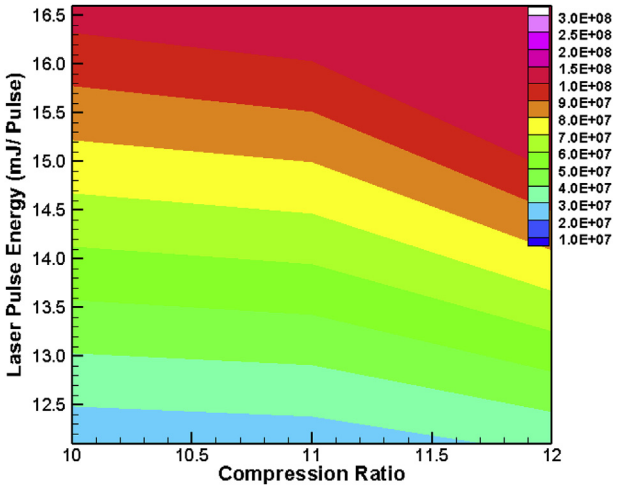

Fig. 10 – Selection of suitable E and CR for lower total particulate numbers emitted by LI hydrogen fueled engine.

Fig. 10 showed the variation of TPN at different Es and CRs. Results showed that TPN was not affected by increasing CR at lower E, though at higher E, increasing CR resulted in higher TPN. Therefore for lower particulate emissions, CR should also be lower. At higher E, increasing CR further enhanced HRR, leading to higher particulate formation.

Conclusions

This experimental study investigated particulate characteristics of laser ignited hydrogen fueled engine, operated with varying LI parameters (E and ST) and engine CR at constant engine speed. To investigate the effect of these parameters, experiment were performed at two different Es (12.1 and 16.6 mJ/pulse), three STs (17, 20 and 23° bTDC) and three CRs (10, 11 and 12) at five different engine loads. Particulate number concentration increased with increasing engine load in all cases. Increasing E resulted in significantly higher particulate number concentrations due to higher HRR, which encouraged incomplete combustion/pyrolysis of the lubricating oil, which was present on the cylinder walls. Increasing E led to significantly higher NMP and AMP number concentrations. Effect of increased number concentration of AMPs was also visible in particulate surface area-size and mass-size distributions, which dominated the AMP regime. Advancing ST resulted in higher NMP number concentration, which decreased with increasing engine load. AMP number concentration decreased for advanced ST. At medium engine loads, TPM increased with advancing ST, though at highest loads, 20° bTDC ST resulted in lowest TPM. Increasing CR resulted in slightly higher particulate number concentrations in both NMP and AMP size regimes. Increasing CR also led to higher particulate surface area and particulate mass. Combined analysis of ST and E showed that lower E and retarded ST resulted in the lowest particulate concentration. Combined analysis of CR and E showed that minimum particulate emissions were obtained at lower CR. At lower CR, variation in E was less effective while at

Please cite this article in press as: Agarwal AK, et al., Effect of laser parameters and compression ratio on particulate emissions from a laser ignited hydrogen engine, International Journal of Hydrogen Energy (2017), http://dx.doi.org/10.1016/j.ijhydene.2017.03.074

higher CR, variation in E was a dominant factor. Overall, it can be concluded from these experimental investigations that particulate emission characteristics of LI hydrogen fueled engine are significantly affected by LI parameters and the CR. Selection of optimum LI parameters and the CR can improve particulate emission characteristics and their potential health effects in case of a LI hydrogen fueled engine.

Acknowledgments

Financial support from SRA scheme of Council for Scientific and Industrial Research (CSIR), Government of India to Dr. Akhilendra Pratap Singh is gratefully acknowledged, which supported his stay at ERL, IIT Kanpur for conducting these experiments.

REFERENCES

[1] Rizwan SA, Nongkynrih B, Gupta SK. Air pollution in Delhi: its magnitude and effects on health. Indian J Commun Med 2013;38(1):4–8.
[2] Gangwar JN, Gupta T, Agarwal AK. Composition and comparative toxicity of particulate matter emitted from diesel and biodiesel fueled CRDI engine. Atmos Environ 2012;46:472–81.
[3] Morakinyo OM, Mokgobu MI, Mukhola MS, Hunter RP. Health outcomes of exposure to biological and chemical components of inhalable and respirable particulate matter. Int J Environ Res Public Health 2016;13(6):592–614.
[4] Jariyasopit N, Zimmermann K, Schrlau J, Arey J, Atkinson R, Yu TW, et al. Heterogeneous reactions of particulate matter-bound PAHs and NPAHs with NO_3/N_2O_5, OH radicals, and O_3 under simulated long-range atmospheric transport conditions: reactivity and mutagenicity. Environ Sci Technol 2014;48(17):10155–64.
[5] Hydrogen Production. U.S. Department of Energy [cited on 25.06.14].
[6] Muradov NZ, Veziroğlu TN. "Green" path from fossil-based to hydrogen economy: an overview of carbon-neutral technologies. Int J Hydrogen Energy 2008;33(23):6804–39.
[7] Subramanian V, Mallikarjuna JM, Ramesh A. Intake charge dilution effects on control of nitric oxide emission in a hydrogen fueled SI engine. Int J Hydrogen Energy 2007;32:2043–56.
[8] Das LM, Mathur R. Exhaust gas recirculation for NOx control in a multicylinder hydrogen-supplemented S.I. engine. Int J Hydrogen Energy 1993;18(12):1013–8.
[9] Gatts T, Li H, Liew C, Liu S, Spencer T, Wayne S, et al. An experimental investigation of H_2 emissions of a 2004 heavy-duty diesel engine supplemented with H_2. Int J Hydrogen Energy 2010;35(20):11349–56.
[10] Zhou JH, Cheung CH, Zhao WZ, Leung CW. Diesel–hydrogen dual-fuel combustion and its impact on unregulated gaseous emissions and particulate emissions under different engine loads and engine speeds. Energy 2016;94(1):110–23.
[11] Zhang B, Ji C, Wang S. Combustion analysis and emissions characteristics of a hydrogen-blended methanol engine at various spark timings. Int J Hydrogen Energy 2015;40(13):4707–16.
[12] Singh AP, Pal A, Agarwal AK. Comparative particulate characteristics of hydrogen, CNG, HCNG, gasoline and diesel fueled engines. Fuel 2016;185:491–9.
[13] Pal A, Agarwal AK. Comparative study of laser ignition and conventional electrical spark ignition systems in a hydrogen fuelled engine. Int J Hydrogen Energy 2015;40(5):2386–95.
[14] Dharamshi K, Pal A, Agarwal AK. Comparative investigations of flame kernel development in a laser ignited hydrogen–air mixture and methane–air mixture. Int J Hydrogen Energy 2013;38(25):10648–53.
[15] Das LM, Dutta V. Hydrogen energy activities in India. Int J Hydrogen Energy 2015;40(11):4280–3.
[16] Salvi BL, Subramanian KA. Experimental investigation on effects of compression ratio and exhaust gas recirculation on backfire, performance and emission characteristics in a hydrogen fuelled spark ignition engine. Int J Hydrogen Energy 2016;41:5842–55.
[17] Srivastava DK, Agarwal AK. Comparative experimental evaluation of performance, combustion and emissions of laser ignition with conventional spark plug in a compressed natural gas fuelled single cylinder engine. Fuel 2014;123:113–22.
[18] Srivastava DK, Dharamshi K, Agarwal AK. Flame kernel characterization of laser ignition of natural gas-air mixture in a constant volume combustion chamber. Opt Lasers Eng 2011;49:1201–9.
[19] Pal A, Agarwal AK. Effect of laser pulse energy on laser ignition of port fuel injected hydrogen engine. Int J Hydrogen Energy 2016;41(1):675–82.
[20] Subramanian V, Mallikarjuna JM, Rames A. Effect of water injection and spark timing on the nitric oxide emission and combustion parameters of a hydrogen fuelled spark ignition engine. Int J Hydrogen Energy 2007;32:1159–73.
[21] Pal A, Agarwal AK. Effect of compression ratio on combustion, performance and emissions of a laser ignited single cylinder hydrogen engine. Int J Hydrogen Energy 2015;40(36):12531–40.
[22] DeBoer PCT, Hulet JF. Performance of a hydrogen-oxygennoble gas engine. Int J Hydrogen Energy 1980;5:439–52.
[23] Mathur HB, Khajuria PK. Performance and emission characteristics of hydrogen fueled spark ignition engine. Int J Hydrogen Energy 1984;9(8):729–35.
[24] Killingsworth NJ, Rapp VH, Flowers DL, Aceves SM, Chen JY, Dibble R. Increased efficiency in SI engine with air replaced by oxygen in argon mixture. Proc Combust Inst 2011;33:3141–9.
[25] Mathur HB, Das LM. Performance characteristics of a hydrogen fuelled S.I. engine using timed manifold injection. Int J Hydrogen Energy 1991;16(2):115–27.
[26] Bünger J, Krahl J, Schröder O, Schmidt L, Westphal GA. Potential hazards associated with combustion of bio-derived versus petroleum-derived diesel fuel. Crit Rev Toxicol 2012;42(9):732–50.
[27] Pope III CA, Thun MJ, Namboodiri MM, Dockery DW, Evans JS, Speizer FE, et al. Particulate air pollution as a predictor of mortality in a prospective study of U.S. adults. Am J Respir Crit Care Med 1995;151:669–74.
[28] Khalek AI, Kittelson DB, Graskow BR, Wei Q, Brear F. Diesel exhaust particle size: measurement issues and trends. SAE Tech Paper 1998;98052.
[29] Liu X, Liu F, Zhou L, Sun B, Schock HJ. Backfire prediction in a manifold injection hydrogen internal combustion engine. Int J Hydrogen Energy 2008;33:3847–55.
[30] Engine exhaust particle Sizer™ spectrometer model 3090. Operation and service manual. USA: TSI; March 2009.
[31] Gupta T, Kothari A, Srivastava DK, Agarwal AK. Measurement of number and size distribution of particles

Please cite this article in press as: Agarwal AK, et al., Effect of laser parameters and compression ratio on particulate emissions from a laser ignited hydrogen engine, International Journal of Hydrogen Energy (2017), http://dx.doi.org/10.1016/j.ijhydene.2017.03.074

emitted from a mid-sized transportation multipoint port fuel injection gasoline engine. Fuel 2010;89(9):2230–3.
[32] Maricq MM, Xu N. The effective density and fractal dimension of soot particles from premixed flames and motor vehicle exhaust. Aerosol Sci 2004;35:1251–74.
[33] Olfert JS, Symonds JPR, Collings N. The effective density and fractal dimension of particles emitted from a light-duty diesel vehicle with a diesel oxidation catalyst. Aerosol Sci 2007;38:69–82.

Please cite this article in press as: Agarwal AK, et al., Effect of laser parameters and compression ratio on particulate emissions from a laser ignited hydrogen engine, International Journal of Hydrogen Energy (2017), http://dx.doi.org/10.1016/j.ijhydene.2017.03.074